

# The effect of $(\text{NH}_4)_2\text{S}_x$ passivation on the (311)A GaAs surface and its use in AlGaAs/GaAs heterostructure devices

D J Carrad<sup>1</sup>, A M Burke<sup>1</sup>, P J Reece<sup>1</sup>, R W Lyttleton<sup>1</sup>, D E J Waddington<sup>1</sup>, A Rai<sup>2</sup>, D Reuter<sup>2</sup>, A D Wieck<sup>2</sup>, A P Micolich<sup>1</sup>

<sup>1</sup>School of Physics, University of New South Wales, Sydney NSW 2052, Australia

<sup>2</sup>Angewandte Festkörperphysik, Ruhr-Universität Bochum, Bochum D-44780, Germany

E-mail: adam.micolich@nanoelectronics.physics.unsw.edu.au

Submitted to: *J. Phys.: Condens. Matter*

**Abstract.** We have studied the efficacy of  $(\text{NH}_4)_2\text{S}_x$  surface passivation on the (311)A GaAs surface. We report XPS studies of simultaneously-grown (311)A and (100) heterostructures showing that the  $(\text{NH}_4)_2\text{S}_x$  solution removes surface oxide and sulfidizes both surfaces. Passivation is often characterized using photoluminescence measurements, we show that while  $(\text{NH}_4)_2\text{S}_x$  treatment gives a 40 – 60× increase in photoluminescence intensity for the (100) surface, an increase of only 2–3× is obtained for the (311)A surface. A corresponding lack of reproducible improvement in the gate hysteresis of (311)A heterostructure transistor devices made with the passivation treatment performed immediately prior to gate deposition is also found. We discuss possible reasons why sulfur passivation is ineffective for (311)A GaAs, and propose alternative strategies for passivation of this surface.

## 1. Introduction

Surface effects increasingly influence transport in electronic devices as they are reduced in size. Understanding the surface's influence and devising methods for minimizing its impact on electronic performance is a vital aspect of device development [1]. Semiconductor surfaces are often non-ideal, featuring complex surface reconstructions and abundant dangling bonds. The latter produce localized energy levels in the surface band structure that can act as metastable trapping sites. GaAs surface states pin the surface Fermi energy near the middle of the band-gap causing surface recombination and difficulties in making ohmic contacts. These present difficulties for GaAs-based devices such as photovoltaic cells and bipolar transistors [2].

Chalcogenide-based passivation has long been investigated towards reducing surface-state problems in III-V semiconductors [1]. A favored route for GaAs surface passivation involves inorganic sulfides such as (NH<sub>4</sub>)<sub>2</sub>S and Na<sub>2</sub>S [3, 4], which remove the native surface oxide and adsorb S onto the Ga and/or As surface atoms. The objective of passivation is to covalently satisfy all Ga and As dangling bonds so that the resulting surface states have energies in either the conduction or valence bands, where they no longer act as charge traps [1, 4, 5]. This ideal is difficult to achieve, and resulted in a plethora of passivation chemistries and treatments in both the liquid and gas phases [1, 6]. Preceding work focussed on basic surfaces such as (100), (110) and (111) due to their applications in device technologies; sulfide passivation of more complex surfaces such as (311)A has not been previously reported. We are interested in (311)A heterostructures as they are an underpinning materials platform for experimental studies of low-dimensional hole systems. Compared to electrons, holes in GaAs have enhanced carrier-carrier interactions due to an increased effective mass and a curious spin- $\frac{3}{2}$  nature due to strong spin-orbit effects. This has resulted in much interest in hole systems for studies of the metal-insulator transition [7, 8], bilayer quantum Hall effect [9, 10], Landé *g*-factor anisotropy [11, 12, 13], anomalous spin-polarization effects [14], 0.7 plateau in quantum point contacts [15], Berry's phase in Aharonov-Bohm rings [16] and the quantum dot Kondo effect [17]. Hole quantum dots are also of interest for quantum computing applications due to a lower spin-decoherence time [18].

We present a study of the efficacy of sulfur passivation treatment of the (311)A GaAs surface, motivated by our previous study on the origin of gate hysteresis in field-effect transistor devices made on p-type Si-doped AlGaAs/GaAs heterostructures [19]. Here we use photoluminescence (PL) and x-ray photoelectron spectroscopy (XPS) measurements to analyze the relative efficacy of sulfur treatment on the (311)A and (100) GaAs surfaces. This is combined with electrical measurements of Schottky-gated transistors made using p-type AlGaAs/GaAs heterostructures and different sulfur passivation treatments to determine the corresponding effect on gate stability. We find that sulfur treatment of the (311)A surface removes the native oxide and replaces it with a sulfide layer, as it does for (100), but does not produce a consistent, corresponding improvement in photoluminescence intensity. We suggest this arises from

the monovalent nature of the Ga dangling bonds at the (311)A surface. Additionally, (NH<sub>4</sub>)<sub>2</sub>S<sub>x</sub> treatment causes a lack of reproducibility in the gate characteristics of AlGaAs/GaAs transistors, likely related to the instability of the As-S bond. We offer potential strategies for improved passivation of the (311)A surface and discuss some practical issues faced in translating sulfur treatments, normally used on bare semiconductor surfaces, to the polymer resist based fabrication typical for transistor devices.

## 2. Methods

The most common approach to III-V semiconductor surface passivation is the use of aqueous (NH<sub>4</sub>)<sub>2</sub>S and (NH<sub>4</sub>)<sub>2</sub>S<sub>x</sub> solutions (see appendix A). These solutions have been successfully applied to device structures ranging from GaAs metal-insulator-semiconductor field-effect transistors (MISFETs) [20] to InAs/GaSb photodiodes [21] to III-V nanowire devices [22]. We considered aqueous and alcoholic solutions of Na<sub>2</sub>S, (NH<sub>4</sub>)<sub>2</sub>S and (NH<sub>4</sub>)<sub>2</sub>S<sub>x</sub>, but mostly restrict ourselves to aqueous solutions due to resist compatibility issues outlined in appendix A, and (NH<sub>4</sub>)<sub>2</sub>S<sub>x</sub>, as the excess sulfur tends to make them more efficacious [23, 24].

Two concentrations of aqueous (NH<sub>4</sub>)<sub>2</sub>S<sub>x</sub> solution were investigated, denoted ‘weak’ and ‘strong’, made from common stock solution prepared by adding 3 mol/L of elemental sulfur (Aldrich) to 20% (NH<sub>4</sub>)<sub>2</sub>S in H<sub>2</sub>O (Aldrich). The stock solution is stirred for several hours until the sulfur is completely dissolved, and stored in a light-free environment to prevent photodecomposition. Strong treatment involves a 10 min sample immersion in  $\sim 5$  mL stock solution. Weak treatment involves 2 min immersion in  $\sim 5$  mL of a 0.5% dilution of stock solution in deionized water. In both cases, passivation solution was heated to 40°C in a water bath [20]. All samples were etched in 31% HCl:H<sub>2</sub>O for 30 s prior to passivation. Prolonged exposure to light and air can result in surface reoxidation [25]; hence devices were stored in the dark between passivation and any subsequent fabrication steps or measurements. We focused on the weak treatment here because etching of the GaAs is sometimes observed [24]. The heterostructures used for the devices have only a thin GaAs cap layer protecting the active AlGaAs and GaAs layers underneath and we wanted to avoid the risk of exposing the AlGaAs, which would oxidize rapidly in air, or generating significant surface roughness due to etching by the (NH<sub>4</sub>)<sub>2</sub>S<sub>x</sub> treatment. We also tested the strong treatment on our devices to check that insufficient treatment solution concentration was not responsible for the lack of passivation efficacy (see section 3.3).

Two types of GaAs substrates were used: epitaxially-grown Si-doped AlGaAs/GaAs heterostructures were used for device fabrication and XPS studies, while ‘bulk’ GaAs substrates without epilayers were used for the PL studies. We used bulk wafer for PL because epilayers interfere with the surface PL signal. The bulk wafers are polished, undoped (semi-insulating) GaAs supplied by AXT. These wafers were also used as the substrate for nominally identical (100)/(311)A AlGaAs/GaAs heterostructures (Bochum

**Table 1.** Samples studied: Bulk GaAs wafer pieces used for PL labeled B1 - B4, Heterostructures without devices used for XPS labeled H1 - H4, Modulation-doped heterostructure devices used for gate hysteresis studies labeled D1 - D6.

Sample	Wafer	Surface	Passivation
B1	bulk	(100)	strong
B2	bulk	(100)	weak
B3	bulk	(311)A	strong
B4	bulk	(311)A	weak
H1	13516a	(100)	none
H2	13516a	(100)	weak
H3	13516b	(311)A	none
H4	13516b	(311)A	weak
D1	13516b	(311)A	none
D2	13473b	(311)A	weak
D3	13516b	(311)A	weak
D4	13473b	(311)A	weak
D5	13516b	(311)A	strong
D6	13516b	(311)A	strong + anneal

13473/13516), custom grown side-by-side in a single deposition using molecular beam epitaxy (MBE). The active region consists of 650 nm undoped GaAs, 35 nm undoped  $\text{Al}_{0.34}\text{Ga}_{0.66}\text{As}$ , 80 nm Si-doped  $\text{Al}_{0.34}\text{Ga}_{0.66}\text{As}$  and a 5 nm undoped GaAs cap. These matched heterostructures have majority carriers of opposite sign – n-type for (100) and p-type for (311)A – due to the amphoteric nature of Si dopants in AlGaAs [26].

Pieces approximately  $3 \times 4 \text{ mm}^2$  were cleaved from the host wafer and cleaned with acetone and 2-propanol. Samples prepared for XPS/PL measurements underwent sulfur passivation as described above, with samples typically measured within 30 min of passivation to avoid surface re-oxidation. For device studies, Hall bars with a height of 130 nm were defined by photolithography and wet etching using a 2 : 1 : 20 buffered HF:H<sub>2</sub>O<sub>2</sub>:H<sub>2</sub>O solution (the buffered HF was 7:1 NH<sub>4</sub>F:HF). Ohmic contacts for (311)A devices were formed by vacuum evaporation of a 150 nm 99:1 AuBe film, followed by annealing at 490°C for 90 s. Schottky gates were defined photolithographically using AZ nLOF2020 photoresist. Sulfur passivation was performed between development and vacuum deposition of 20 nm Ti / 80 nm Au gate metal. Passivated samples were stored under deionized H<sub>2</sub>O during transfer to the evaporator, and exposed to air for < 5 min before the evaporator chamber reached vacuum (< 1 mTorr). Significant surface reoxidation should not arise from such brief air exposure [25], as confirmed by PL in appendix B. We expect the passivated surface to remain robust after metal deposition as the gate metal protects the surface from light/air. Table 1 lists the samples/devices studied along with the wafer type, surface orientation and passivation treatment used.

Room temperature PL and XPS measurements were used to compare the action

of the (NH<sub>4</sub>)<sub>2</sub>S<sub>x</sub> passivation solution on the (311)A GaAs surface with what is known/expected for (100) GaAs surfaces. The PL excitation was provided by a 488 nm Ar ion laser (Coherent Innova 70). Luminescence was coupled to a 0.27m grating spectrometer (J/Y SPEX 270M) and recorded by CCD, giving a spectral resolution of 3 nm. The PL apparatus has 1 mW incident power, giving 0.49 W/mm<sup>2</sup> intensity at focus. PL spectra are normalized to the peak intensity of a corresponding unpassivated reference sample. XPS measurements were performed using a ThermoScientific ESCALAB250Xi system with a monochromated Al K $\alpha$  source ( $h\nu = 1486.68$  eV at 164 W power). A 500 nm spot size and 90° photoelectron take-off angle were used. The C(1s) peak at 285.0 eV is the binding energy reference for all measurements, which are expected to be accurate to  $\pm 0.1$  eV. The Avantage software package was used for XPS peak fitting.

Standard four-terminal ac lock-in techniques were used for the electrical studies, which were performed at  $T = 4.2$  K in liquid He. The drain current  $I_d$  was measured with applied source-drain bias  $V_{sd} = 100$   $\mu$ V at a frequency  $f = 73$  Hz. A dc gate bias  $V_g$  was applied using a Keithley 2400 to enable monitoring/limiting of the gate leakage current  $I_g$ .

### 3. Results

#### *3.1. XPS study of the effect of (NH<sub>4</sub>)<sub>2</sub>S<sub>x</sub> on the (311)A GaAs surface*

We first discuss XPS studies of bare and passivated (311)A GaAs surfaces. The surface sulfidization chemistry for bare and passivated (100) GaAs surfaces is well characterized using XPS [28, 29, 27, 30, 31, 32, 33, 34]. We prepared and measured bare and passivated (100) reference surfaces in parallel with (311)A surfaces to provide more direct comparison, and to better isolate the effect of surface orientation on passivation chemistry. XPS data for passivated and unpassivated samples is shown in figure 1(a/c/e) and (b/d/f) for (100) and (311)A, respectively. Beginning with the As(2p<sub>3/2</sub>) core level spectra in figure 1(a/b), the unpassivated surfaces show peaks corresponding to GaAs (1323.2 eV) and As<sub>2</sub>O<sub>3</sub> (1326.3 eV) for both orientations. After passivation, the As<sub>2</sub>O<sub>3</sub> peak was eliminated and a small peak (1324.5 eV) corresponding to disulfide bridges was observed [27]. The disulfide peak emerges to an equivalent extent for (100) and (311)A. Turning to the Ga(2p<sub>3/2</sub>) spectra in figure 1(c/d), the unpassivated surfaces show peaks corresponding to GaAs (1117.4 eV) and Ga<sub>2</sub>O<sub>3</sub> (1118.5 eV). The Ga<sub>2</sub>O<sub>3</sub> peak intensity for (100) is  $\sim 2\times$  that for (311)A. This likely reflects the single dangling bond nature of surface Ga atoms on (311)A [35, 36]. There is a clear Ga peak, and a weaker peak at higher energy for the passivated surfaces that may correspond to Ga-S bonding or residual Ga<sub>2</sub>O<sub>3</sub>. Unfortunately, the low peak intensity makes conclusive assignment of these peaks' sources difficult. Turning to the combined Ga(3s)/S(2p) spectra in figure 1(e/f), the unpassivated surface gives two peaks at 156.4 and 160.4 eV corresponding to GaAs bonds. The passivated samples show additional small peaks at

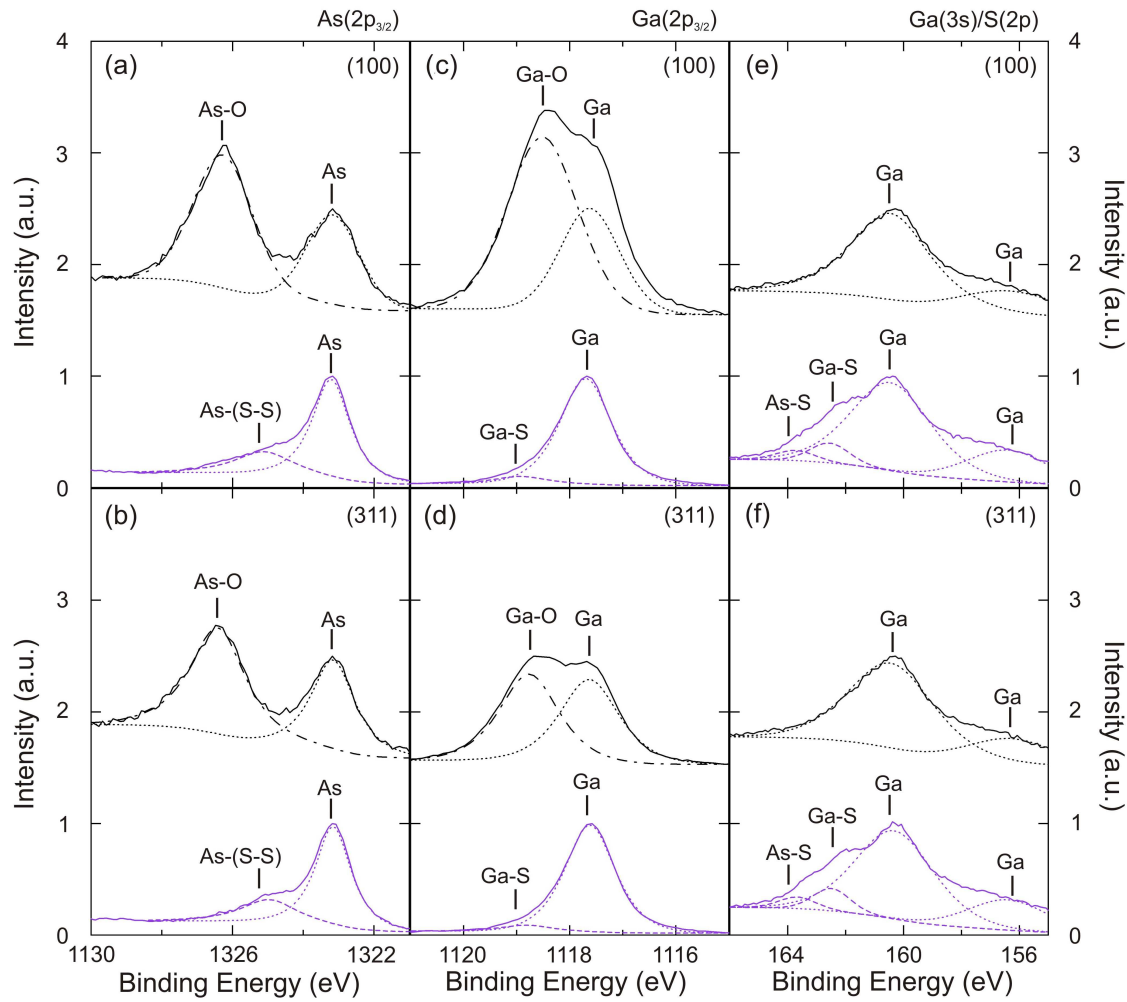


**Figure 1.** (a,b) As(2p<sub>3/2</sub>), (c,d) Ga(2p<sub>3/2</sub>) and (e,f) Ga(3s)/S(2p) XPS core level spectra for passivated (purple) and unpassivated (black) GaAs surfaces with (100) (top row) and (311)A (bottom row) orientation. Intensity is normalized to the Ga-As peak in each case, with unpassivated intensities offset vertically by 1.5 for clarity. Solid lines are the measured spectra, dotted and dashed lines are peak fits for the Ga-As and X-Y spectral peaks, where X = Ga,As and Y = S,O, respectively.

163.3 and 162.1 eV that are likely As-S and Ga-S bonds (expected at 163.2 and 162.3 eV), respectively [37]. An alternate possibility is that one of these peaks corresponds to a disulfide bridge (expected at 163.5 eV). Ultimately, the strong similarities between the XPS spectra for (311)A and (100) suggest that the passivation treatment removes surface oxide and establishes a surface sulfide layer with roughly equivalent efficacy and chemistry.

### 3.2. Comparative photoluminescence study of $(\text{NH}_4)_2\text{S}_x$ treated (100) and (311)A GaAs surfaces

A corresponding equivalence was not observed in the PL measurements. Figure 2 shows PL spectra for (a) the (100) and (b) the (311)A surfaces after passivation with the

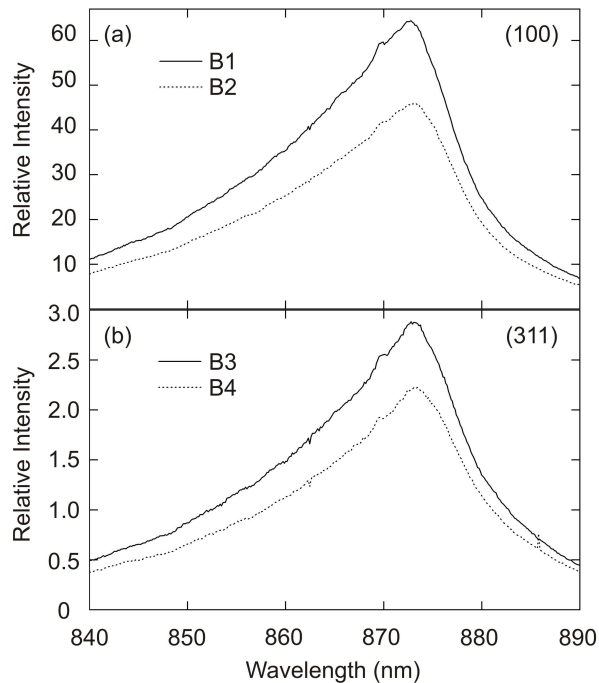


**Figure 2.** PL intensity vs wavelength for (a) Samples B1 and B2 with (100) surfaces passivated with strong (solid line) and weak (dotted line) solution, respectively, and (b) Samples B3 and B4 with (311)A surfaces passivated with strong (solid line) and weak (dotted line) solution, respectively. The intensity is normalized to PL spectra for an untreated sample with matching surface orientation.

strong and weak  $(\text{NH}_4)_2\text{S}_x$  solutions. In each case, the intensity is normalized to the peak intensity for an unpassivated surface with matching orientation (see appendix C), and represents the factor by which passivation increases the PL intensity. Passivation increases the PL intensity by only 2 – 3 $\times$  for (311)A GaAs, compared to 40 – 65 $\times$  for (100) GaAs, suggesting passivation is much less effective on (311)A GaAs. This likely arises from Ga, which presents a double-dangling bond for (100) and a single-dangling bond for (311)A, unlike As, which presents a double-dangling bond on both surfaces [35, 36]. Although the Ga-S and As-S XPS peaks show no difference between (100) and (311)A in figures 1(e/f), the different Ga dangling bond valence for (311)A may mean that sulfur atoms are unable fully satisfy all Ga dangling bonds. This could explain the lower PL intensity observed for (311)A in figure 2(b). We discuss this further in section 4.

The electrical data in section 3.3 is obtained at low temperature, and the question could be asked: What about the PL at low temperature? The difficulty is that PL does not just measure surface recombination; it is also influenced by bulk radiative transitions within the excitation photon penetration depth. Additional peaks emerge in the PL at low  $T$  corresponding to radiative transitions not observed at 300 K. These obscure the underlying band-to-band PL peak used to assess surface recombination. Nevertheless, one can compare the absolute PL intensity for passivated and unpassivated surfaces.

Skromme *et al* [38] did this for (100) GaAs at  $T = 300$  and 1.8 K. They observed  $100 - 2800\times$  increases in PL intensity at 300 K upon passivation, dependent on sample doping, but a  $\sim 3.5\times$  *reduction* in passivated sample PL intensity at 1.8 K. Their ultimate conclusion was that “recombination associated with the bare surface does not limit the lifetime at low temperature as it does at 300 K.” In other words, surface-states no longer dominate recombination at low  $T$ , other recombination centers do. This does not mean that the surface-states are removed, nor that they are no longer electrically active; it is more that low  $T$  PL is a poor probe of surface-states.

For completeness, we repeated the PL study for (311)A GaAs surfaces at  $T = 10$  and 20 K: p-type AlGaAs/GaAs heterostructure devices still exhibit qualitatively similar gate instability at these temperatures [19]. The band-to-band recombination peak intensity increased by  $\sim 4\times$  for (311)A GaAs with the weaker  $(\text{NH}_4)_2\text{S}_x$  solution applied. As Skromme *et al* [38] point out, such a small change is generally considered negligible in a PL measurement. In particular, the increase is small compared to the  $40\times$  increase in band-to-band peak intensity obtained for passivated (100) GaAs obtained at room temperature. Ultimately, our conclusion matches Skromme *et al*. [38]: low  $T$  PL is a poor probe of surface-states. We instead turn to heterostructure devices to further examine (311)A surface passivation.

### 3.3. Effect of passivation on gate hysteresis in (311)A heterostructure devices

Gated Hall bars made using Si-doped (311)A AlGaAs/GaAs heterostructures display strong gate hysteresis with an anticlockwise hysteresis loop in the  $I_d$  versus  $V_g$  characteristics. This hysteresis is consistent with trapping of net negative charge between the gate and the 2DHG, either in surface-states or the modulation doping layer [19]. Figure 3(a) shows a typical hysteresis loop obtained from an unpassivated (311)A device. The most striking feature is the long plateau at intermediate  $V_g$  whilst sweeping to positive  $V_g$ . Here, 2DHG depletion is strongly suppressed due to surface-state charge trapping and/or dopant layer charge migration. Depletion resumes for sufficiently positive  $V_g$ , and in most Schottky-gated devices we studied, pinch-off (i.e.,  $I_d = 0$ ) is attained before  $V_g > +1$  V. The  $I_d$  plateau length and pinch-off voltage  $V_p$  provide a measure of charge trapping/migration within the device. Hence an effective surface passivation should result in reduced  $I_d$  plateau length and lower  $V_p$ . Note that  $I_d$  versus  $V_g$  is a reasonable approximation to a capacitance-voltage (C-V) study because  $I_d$  depends upon the insulator capacitance. MOS capacitor C-V studies are just a simpler route to studying insulator trapping that removes the need for an FET conducting channel.

Figures 3(b-f) show electrical characteristics for passivated devices D2-D6. The results for the weak passivation solution vary, with the  $I_d$  plateau extending (fig. 3(b)), shortening (fig. 3(c)), and in one case, disappearing entirely (fig. 3(d)). The behaviour in figure 3(b/c) is most typical; across the five devices we observe  $V_p = +0.25 - +0.8$  V and plateau lengths up to 0.4 V. We have been unable to reproduce the outcome for device

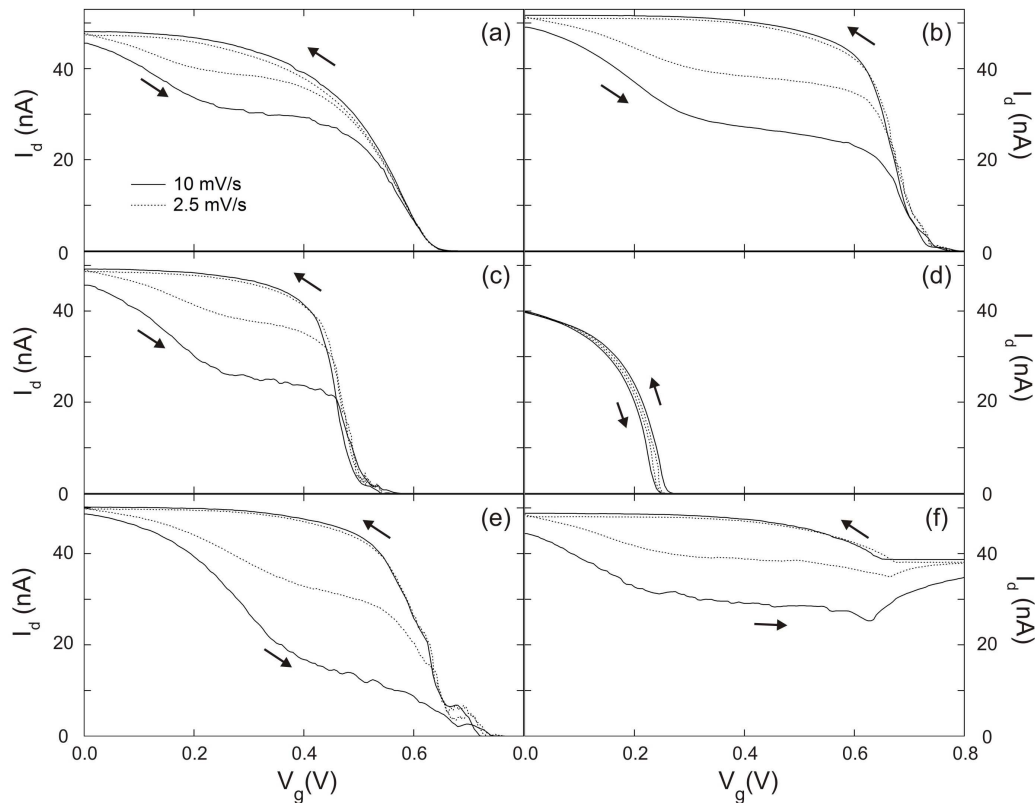


**Figure 3.** Drain current  $I_d$  vs gate bias  $V_g$  for Devices (a) D1 - unpassivated, (b-d) D2-D4 - weak passivation, (e) D5 - strong passivation and (f) D6 - strong passivation and a post-passivation anneal at 360°C for 10 min under Ar. The arrows indicate sweep direction (upsweep/downsweep); the solid (dashed) lines indicate  $V_g$  sweep rates of 10(2.5) mV/s, respectively. Pinch-off could not be achieved for Device D6; the gate leaks strongly as  $V_g \rightarrow +0.6$  V. The  $I_d$  rise for  $V_g > +0.61$  V (upsweep), and  $I_d$  plateau on return to  $V_g = +0.61$  V (downsweep) represent the current limiting action of the  $V_g$  source, which holds  $V_g = +0.61$  V for all set  $V_g > +0.61$  V where  $I_g > 50$  nA.

D4 (fig. 3(d)) in a second device despite numerous attempts; yet the characteristics in fig. 3(d) were repeatable for subsequent cooldowns of device D4. A more focussed surface chemistry study may identify a route for producing the desirable outcome in fig. 3(d) more consistently.

A possible argument for the inconsistent results in fig. 3(b-d) is an insufficiently strong passivation treatment. Figure 3(e) shows results from an attempt to more effectively passivate the GaAs surface. Device D5 was prepared using the 200 $\times$  more concentrated passivation solution, and although the  $I_d$  plateau at intermediate  $V_g$  is weakened, there is little reduction in  $V_p$  and the device becomes more unstable at low  $I_d$ . This suggests that the inefficacy of passivation treatment on the hysteresis is not related to insufficient sulfidization.

Post-passivation annealing is an informative experimental tool because the large difference in Ga-S and As-S bond stability [39] means annealing increases Ga-S bonding

at the expense of As-S surface bonds [30, 40, 41]. Little is known about the sulfur chemistry of the (311)A surface, but since (311)A surface As atoms are (100)-like (see section 4), we assume that desorption of As surface bonds is complete for samples annealed above 350°C [32, 41, 42]. Device D6 was prepared using the strong solution followed by a post-passivation anneal for 10 min at 360°C to determine the influence As-S bonds have on the electrical characteristics. The entire anneal process was conducted at 1 atm Ar to prevent oxidation, with photo-processing and metallization performed as soon as practicable thereafter. The robustness of passivation to subsequent photo-processing is discussed in appendix B.

Post-passivation annealing appears detrimental for the (311)A surface; as figure 3(f) shows, pinch-off cannot be achieved in these devices. The  $I_d$  plateau on sweeping to positive  $V_g$  begins at a lower  $V_g$  and extends such that  $I_g$  exceeds the 50 nA limit set by the gate voltage source before the end of the  $I_d$  plateau (c.f. figure 2 of [19]). The lack of depletion in figure 3(f), particularly at low  $V_g$ , suggests that surface As-X bonds may play an important role in the hysteresis. The corollary is that As-S bonding may give reduced hysteresis, which may explain the hysteresis-free behaviour in device D4. The variability in passivation efficacy found in figures 3(b)-(d) may also be symptomatic of low As-S bond stability [39, 40], which leads to surface As accumulation and As-As and As-O surface bond formation with H<sub>2</sub>O washing [33, 42, 43]. This would make aqueous passivation treatments a more capricious and variable prospect compared to gaseous treatments, for example. Gates on (311)A that underwent post-passivation annealing also tend to be more leakage prone. This may arise from Be diffusion from the ohmic contacts; the contacts are deposited and annealed prior to the passivation and post-passivation anneal. Although the post-passivation anneal is 130°C lower in temperature than the ohmic contact anneal, its duration is more than six times longer. The rapid diffusion and surface aggregation of Be in GaAs is well known [44].

Returning briefly to device D4, one possibility is that passivation has produced a sharp reduction in the low energy tail of the surface-state spectrum or the spectrum has changed such that a large subset of the surface-states local to the surface Fermi energy of the untreated surface was shifted in energy (i.e., passivation induces a change in band-bending). In both cases, reduced charge trapping at low  $V_g$  would cause rapid depletion, allowing pinch-off before onset of the  $I_d$  plateau. A partially effective passivation may be sufficient to achieve this. Device D4, although a one-off example, indicates that a passivation treatment that can significantly reduce the gate hysteresis in (311)A heterostructure devices may exist.

#### 4. Discussion

Drawing together the XPS, PL and electrical measurements above, it is evident (NH<sub>4</sub>)<sub>2</sub>S<sub>x</sub> treatment removes oxide and sulfidizes the surface for both orientations. The PL intensity enhancement is smaller for (311)A, and there is little corresponding improvement in gate hysteresis for (311)A-based FET devices. We embarked on this

study expecting that sulfur passivation may lessen the gate hysteresis; we are instead left with several questions: Why does (NH<sub>4</sub>)<sub>2</sub>S<sub>x</sub> produce a clear chemical change for (311)A with little improvement in PL intensity and gate characteristics? Is there something about the (311)A surface that would make this expected behaviour? Is there some insight for how a more effective passivation treatment might be formulated? We now attempt to answer these questions.

Higher-Miller-index surfaces present as linear combinations of lower-Miller-index surfaces. The (311) surface can be considered the average of (100) and (111) surfaces. [26, 45] The (311)A surface studied here ideally presents equal densities of (100)-like As double-dangling bonds and (111)A-like Ga single-dangling bonds. We propose that the (311)A surface's bimolecular nature is central to the inefficacy of sulfur passivation despite the clear sulfur binding evident by XPS (figure 1). For clarity of later discussion, we first briefly address how (NH<sub>4</sub>)<sub>2</sub>S<sub>x</sub> treatment affects surface Ga and As atoms for (100) and (111)A.

(NH<sub>4</sub>)<sub>2</sub>S<sub>x</sub> treatment produces a surface containing Ga-S, As-S and surface-bound S-S dimers; however due to the reduced stability of the As-S bond [39, 40], a H<sub>2</sub>O rinse leaves mostly Ga-S bonds with remaining surface-bound S forms washed away [33, 43]. Thermal annealing exacerbates the dominance of Ga-S bonds [30, 31, 40], making the Ga-S bond the logical first consideration. For (100), the Ga-bound S atom adopts a Ga-S-Ga bridge configuration [46, 47] to satisfy the surface Ga double-dangling bond. Total energy calculations using density-functional theory suggest the resulting bonding and antibonding orbitals for Ga-S bonds sit within the valence and conduction bands [48]. This should produce a substantial reduction in Ga-related mid-gap surface-state density, and depinning of the surface Fermi level. Indeed, a substantial reduction in Ga-related surface state density close to the conduction band was reported for capacitance-voltage (C-V) and deep level transient spectroscopy (DLTS) studies of passivated (100) surfaces [2, 20, 23]. In contrast, for (111)A, the Ga-bound S atom sits above the surface Ga atom to satisfy the surface Ga single-dangling bond [49, 50, 51]. Calculations suggest the bonding and anti-bonding orbitals sit inside the band-gap in this case [52]. Hence Ga-related mid-gap states for unpassivated (111)A are replaced by Ga-S states nearer the valence band for passivated (111)A. This should cause the surface Fermi energy to pin closer to the valence band maximum rather than depinning [52]. That said, experiments suggest the surface Fermi energy moves away from the valence band maximum upon (111)A passivation [51], possibly due to S substituting some uppermost sub-surface As atoms in addition to bonding to surface Ga. Either way, passivation efficacy for (111)A would be diminished compared to (100) [51].

The behaviour of surface As is more difficult because although surface As for (311)A is (100)-like and passivation for (100) has been heavily studied, the role of As-S bonding in passivation for (100) remains poorly understood. For example, some theoretical studies suggest the As-S antibonding state for (100) sits within the band-gap [48, 52], while others place these states within the valence band [53]. The role and importance of As-S bonding is also debated on the experimental side. Some suggest As-S and As-(S-S)

are central to passivation [29, 32, 54], others that Ga-S bonds are key [33, 41, 42], and some that both Ga-S and As-S bonds are involved [55]. One difficulty is the relative As-S bond weakness and tendency for surface As accumulation, which causes additional mid-gap levels [42].

We now consider (311)A specifically: In essence, (311)A is a worst case scenario. First, the Ga dangling bonds are (111)-like and Ga-S bonding should produce states within the band-gap [45, 52]. This could explain the lack of PL intensity increase for the sulfidized (311)A surface. Second, (311)A should display equal proportions of Ga and As dangling bonds [26, 45]. This means that (311)A surface passivation will always be difficult; compromised by the As-S bond's weakness to H<sub>2</sub>O exposure [33, 42, 43]. An action as simple as changing the rinse time could alter the As-S bonding, giving different gate characteristics to each device, as in fig. 3. Finally, the (311)A surface can display metastable reconstructions [56]; this may further complicate the surface chemistry and electronic states. This explanation for the passivation inefficacy of (311)A is simplistic, further theoretical and surface studies would significantly enhance understanding. Studies of (311)A surface-state spectrum using frequency dependent C-V [23, 55] or DLTS [2] would also be valuable.

The final question is whether a formulation exists that might passivate (311)A more effectively. The problem here is that both the Ga and As surface atoms need attention. The problem with (311)A surface Ga is that the dangling bond is monovalent and sulfur is divalent. A monovalent adsorbate, e.g., Cl, is one alternative. HCl passivation of (111)A has been demonstrated [57], but we found no improvement for (311)A heterostructure devices by HCl treatment. Recent studies have shown that post-chloridation thermal annealing, possibly combined with hydrazine treatment, can significantly enhance Cl passivation efficacy by removing excess As [58]. Further studies of more complex Cl treatments for (311)A would be of interest. Turning now to dangling As bonds, an obvious alternative is Se, with several reports that it is more effective and stable against oxidation than S treatment [59, 60]. The greater subsurface penetration of Se [34, 61, 62] may also be favorable assuming an As antisite defect model [63] for GaAs surface states. Possible formulations include Na<sub>2</sub>Se in NH<sub>4</sub>OH followed by Na<sub>2</sub>S<sub>(aq)</sub> [59], SeS<sub>2</sub> in CS<sub>2</sub> [60] or Se-loaded (NH<sub>4</sub>)<sub>2</sub>S [64]. Note that this would only deal with surface As; passivation of (111)-like surface Ga bonds would entail additional treatment. Ultimately, As-chalcogen bond stability and surface As accumulation may still be an issue even with Se-passivation.

Engineering of the heterostructure's cap layer may be the most viable alternative. This would involve growing a degenerately-doped GaAs cap layer [19]. This cap could be partitioned by wet-etching to form gates for the device, as in undoped Heterostructure Insulated Gate Field Effect Transistors (HIGFETs) [65, 66], although the device would still operate as 'normally on' due to the Si modulation doping layer. The advantage is that the the highly-conductive cap screens the conducting channel from the surface-states; the disadvantage is that it requires far more complex device processing.

We finish by commenting on the implications for C-doped (100)-oriented

AlGaAs/GaAs heterostructures [67, 68, 69, 70, 71], where gate hysteresis is also observed. We expect the hysteresis in these heterostructures to arise mainly from dopant fluctuations [19]. We observe no hysteresis in (100) Si-doped electron devices, which suggests surface states have a similarly small impact on (100) C-doped hole devices. Nevertheless, some non-linearity is seen in our (100) electron devices at low  $V_g$ , which we tentatively assign to surface states (see, e.g. figure 3 of [19]). A study of sulfur passivation of both electron and hole (100) devices with may be useful; one would expect better passivation here since (100) only presents Ga double-dangling bonds, which are robustly passivated by sulfidization. The literature on passivation of (100) GaAs supports this, but perfect passivation is not achievable, even for (100) GaAs. One aspect to note is that a HfO<sub>2</sub> insulator between gate and heterostructure surface is often used to prevent (apparent) gate leakage in p-type AlGaAs/GaAs heterostructures [19, 70]. This may adversely affect passivation treatment as the organometallic precursors used in atomic layer deposition (ALD) attack the GaAs surface [72]. Although the relative concentration of Ga-S bonds remained relatively unaffected in ALD deposition of Al<sub>2</sub>O<sub>3</sub> on (NH<sub>4</sub>)<sub>2</sub>S passivated (100) GaAs [73], it is unclear whether this would hold for HfO<sub>2</sub> deposition. HfO<sub>2</sub> insulated C-doped (100) AlGaAs/GaAs devices also display gate hysteresis [70], but to a much lesser extent than (311)A devices [19]. It would be interesting to study the effect of sulfur passivation of C-doped (100) AlGaAs/GaAs devices, as it may enable the highly-stable devices needed for studying the fundamental physics of low-dimensional hole systems.

## 5. Conclusions

We studied the efficacy of (NH<sub>4</sub>)<sub>2</sub>S<sub>x</sub> surface passivation treatment as a prospective solution to the gate hysteresis problem in nanoscale devices made using (311)A AlGaAs/GaAs heterostructures. XPS studies on (311)A and (100) heterostructures grown simultaneously by MBE show very similar surface chemistry for both surface orientations. PL measurements showed an improvement in PL intensity by 40 – 65× and 2 – 3× for (100) and (311)A surfaces, respectively, relative to untreated surfaces. The comparative lack of PL intensity increase for (311)A is consistent with a lack of reproducible improvement in gate hysteresis (311)A FET devices made with the passivation treatment performed immediately prior to gate deposition. We suggest that inefficient passivation, despite an obvious change in the surface chemistry, arises due to the mixture of monovalent Ga and divalent As dangling bonds present on the (311)A surface. We expect monovalent Ga to be unpassivated by S – giving at best a small increase in PL intensity – and divalent As-S bonds to be unstable, which could explain the lack of reproducibility in gate characteristics for (311)A devices. Further work on (311)A surface passivation is encouraged and could include Cl- or Se-based treatments, or the addition of a GaS or degenerately-doped GaAs cap layer as alternative passivation strategies.

## Acknowledgments

This work was funded by Australian Research Council Grants DP0877208, FT0990285 and DP110103802. DR and ADW acknowledge support from DFG SPP1285 and BMBF QuaHL-Rep 01BQ1035. This work was performed in part using the NSW node of the Australian National Fabrication Facility (ANFF) and the Mark Wainwright Analytical Center at UNSW. We thank Dr Bill Bin Gong for performing the XPS measurements reported here, Tim Bray for assistance with some PL measurements, and Tim Bray, Alex Hamilton and Oleh Klochan for helpful discussions.

## Appendix A. Practicality of incorporating (NH<sub>4</sub>)<sub>2</sub>S<sub>x</sub> passivation into device processing

A range of possible sulfur treatment formulations exist, we focussed on Na<sub>2</sub>S and (NH<sub>4</sub>)<sub>2</sub>S based solutions as they provide the best mix of ease and effectiveness. While Na<sub>2</sub>S passivation is reported to be more robust to light/oxygen than (NH<sub>4</sub>)<sub>2</sub>S [27], treatment with (NH<sub>4</sub>)<sub>2</sub>S gives complete oxide removal and a more sulfidized surface with no traces of Na [29, 40]. This behaviour can be enhanced by adding elemental S i.e., treating with (NH<sub>4</sub>)<sub>2</sub>S<sub>x</sub> [23, 24]. Thus, aqueous (NH<sub>4</sub>)<sub>2</sub>S and (NH<sub>4</sub>)<sub>2</sub>S<sub>x</sub> solutions are commonly used for passivation of structures ranging from GaAs metal-insulator-semiconductor field-effect transistors (MISFETs) [20] to InAs/GaSb photodiodes [21] to III-V nanowire devices [22].

To incorporate S passivation into device processing, it was essential that treatment left the photoresist intact to facilitate deposition of a photolithographically-defined gate such as in figure A1(a) and (c). Hence we began by studying the photoresist compatibility of various sulfur passivation treatments including aqueous Na<sub>2</sub>S and (NH<sub>4</sub>)<sub>2</sub>S stock solutions diluted in 2-propanol, 2-methyl-2-propanol (t-butanol) and H<sub>2</sub>O. We studied three different resists: MicroChem S1813, a positive photoresist; AZ nLOF2020, a negative photoresist; and MicroChem 950k polymethylmethacrylate (PMMA), a positive electron-beam lithography (EBL) resist.

While alcoholic passivation is often more effective [25], photoresist tends to be alcohol soluble. A developed photoresist pattern began to dissolve within a few seconds of immersion in a 2% solution of (NH<sub>4</sub>)<sub>2</sub>S<sub>x</sub> stock solution in 2-propanol. The photoresist was completely removed after 15 s, a period insufficient for effective passivation of any exposed GaAs. Similar results were obtained for stock solution diluted in 2-methyl-2-propanol; an example where gate deposition was attempted after passivation is shown in figure A1(b). Clearly the gate has not formed properly, with gate metal covering large regions suffering unintentional photoresist removal during passivation. PMMA proved more favorable due to its low solubility in 2-propanol. Patterned PMMA films remained intact for immersions of up to 15 min in (NH<sub>4</sub>)<sub>2</sub>S<sub>x</sub> stock solution in 2-propanol. Although this immersion time is sufficient for effective passivation, electron-beam lithography is impractical for large area devices. Qualitatively similar results to the above were

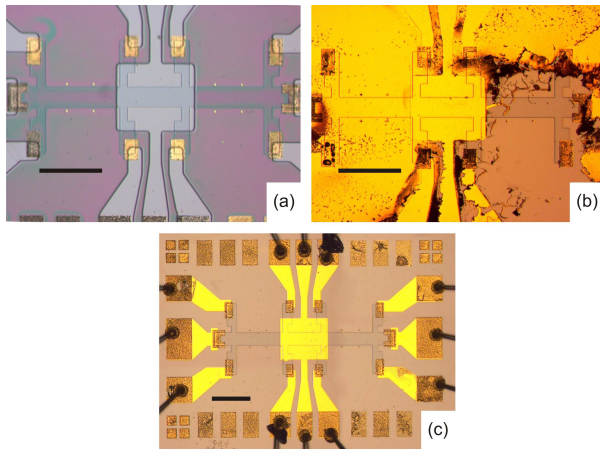


**Figure A1.** Optical micrographs of a device (a) before passivation and gate deposition and (b) after passivation with a 2-methyl-2-propanol solution and gate deposition. (c) shows a successful device for reference. The outline device center is a 130 nm high hall bar mesa, the grainy gold regions are annealed AuBe ohmic contacts and the bright yellow regions are Ti/Au gates and leads. In (a), the purple region is the developed resist. In (b), the gate metal is poorly defined due to the photoresist being damaged by the alcohol passivation solution. The black scale bars in all images represent 300  $\mu\text{m}$ .

obtained for  $\text{Na}_2\text{S}$  solutions in 2-propanol and 2-methyl-2-propanol.

Turning now to purely aqueous solutions, we found a marked difference between  $\text{Na}_2\text{S}$  and  $(\text{NH}_4)_2\text{S}_x$  based solutions for photoresist films. Photoresist films remained intact for at least 5 min. for  $(\text{NH}_4)_2\text{S}_x$ , whereas significant resist damage resulted in  $< 30$  s for  $\text{Na}_2\text{S}$  based solutions. Resist damage was widespread for  $\text{Na}_2\text{S}$  solutions but concentrated at the pattern edges. We suspect this occurs because  $\text{Na}_2\text{S}$  is a much stronger base than  $(\text{NH}_4)_2\text{S}_x$ ; UV-exposed photoresist is normally developed in tetramethylammonium hydroxide (TMAH), which is also basic. We performed the remainder of the studies in aqueous  $(\text{NH}_4)_2\text{S}_x$ , since it was the only passivation solution for which both photo- and EBL-resists remain intact for long immersions.

## Appendix B. Initial characterization of passivation solutions and their robustness

After establishing the suitability of the aqueous  $(\text{NH}_4)_2\text{S}_x$  solutions, we used PL measurements on (100) GaAs to confirm their efficacy. The passivated samples used are listed in Table B1. Figure B1(a) shows PL intensity versus wavelength for Sample B5 treated with the strong solution and Sample B6 treated with the weak solution. The PL intensity is normalized to that obtained from an otherwise equivalent untreated sample. A  $\sim 40\times$  and  $\sim 90\times$  increase in PL intensity was observed for Samples B5 and B6, respectively. The  $2.25\times$  improvement in PL intensity produced by increasing passivation solution concentration by  $\sim 200\times$  is small compared to the  $40\times$  increase in PL intensity produced using the weak solution. Regarding the appearance of treated

**Table B1.** List of samples discussed in the appendices. All are bulk, passivated GaAs wafer pieces used for PL.

Sample	Wafer	Surface	Passivation
B5	bulk	(100)	strong
B6	bulk	(100)	weak
B7	bulk	(100)	strong
B8	bulk	(100)	weak
B9	bulk	(100)	weak + photoprocessed

surfaces, Nannichi *et al* [24] report deposition of a thin off-white precipitate film on the GaAs surface after  $(\text{NH}_4)_2\text{S}_x$  passivation. We only obtain this when the wafer is removed directly from the strong solution. This could be prevented by diluting this solution with  $\text{H}_2\text{O}$  prior to removing the sample. We found no appreciable change in PL intensity when using this dilution method for preventing sulfide film formation.

We also used PL to study the robustness of the treatment under different storage conditions. Figure B1(b) shows that the PL intensity for B7 was only 15% lower after 1 week stored in the dark under room atmosphere conditions than immediately after passivation. This is within the experimental error for a PL measurement, suggesting little/no degradation of the passivation. This confirms the brief air exposure between passivation and gate deposition for devices D2-D5 is unlikely to adversely affect performance. It can be desirable to thermally anneal the sample to  $\sim 350^\circ\text{C}$  after passivation; patterned resists are generally destroyed at such temperatures. This would require passivation and annealing prior to resist deposition, thus we also studied the robustness of a passivated surface to subsequent photolithographic processing. Samples B8 and B9 were passivated together, we then deposited an AZ nLOF2020 resist film on B9, baked it at  $110^\circ\text{C}$  for 60 s and developed in TMAH. Sample B9 was not irradiated with UV prior to development as the surface underneath the gates is normally protected by the photomask during exposure. The PL intensity was not reduced by the addition of photoprocessing steps, as shown in figure B1(c). This confirms device D6 should remain passivated during gate photoprocessing/deposition.

### Appendix C. Raw PL data of unpassivated (100) and (311)A GaAs surfaces

The data in figure 2(a/b) were normalized to the peak of untreated (100)/(311)A oriented GaAs, respectively. Figure C1 shows the raw intensity for these reference samples. The data in figure C1 has not been normalized unlike all other presented PL data; the intensity here refers to the recorded intensity incident on the CCD camera. Note also that the (100) reference sample in figure C1 is not the same that in appendix B; each experiment had its own unique reference sample and this data is from reference samples used in conjunction with the data in figure 2. Reference and passivated samples were cleaved from adjacent positions on the host wafer to ensure optimum similarity.

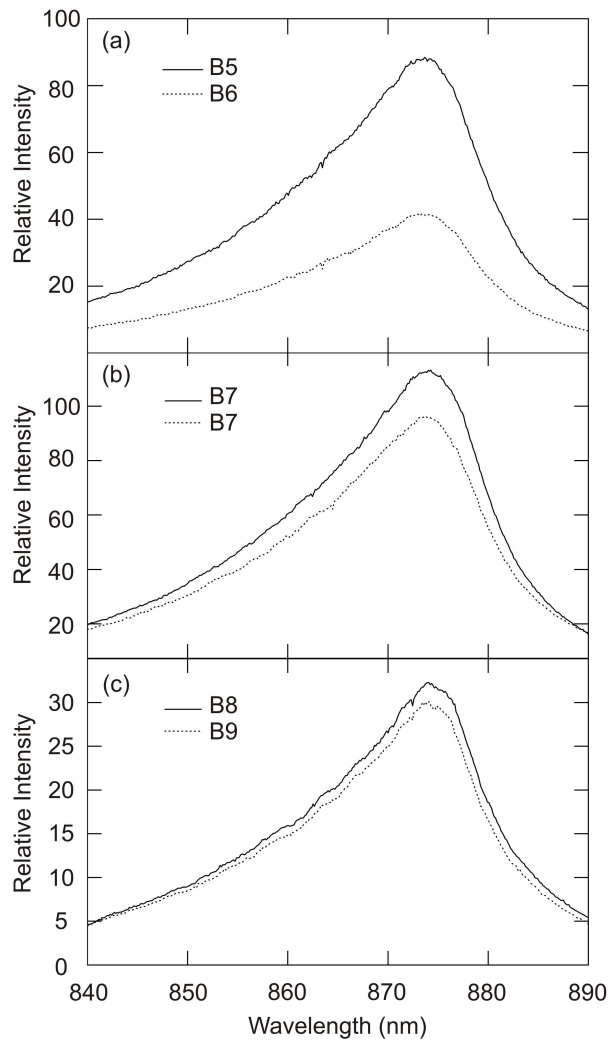


**Figure B1.** (a) PL intensity versus wavelength for Samples B5 and B6. Yields are normalized using the PL spectrum obtained from an otherwise equivalent untreated sample. (b) PL spectrum of Sample B7 obtained immediately after passivation (solid line) and after one week (dashed line) of storage in the dark under room atmosphere conditions. (c) PL spectrum of Samples B8 and B9 showing that comparable PL intensities are obtained whether or not the sample is photoprocessed after passivation.

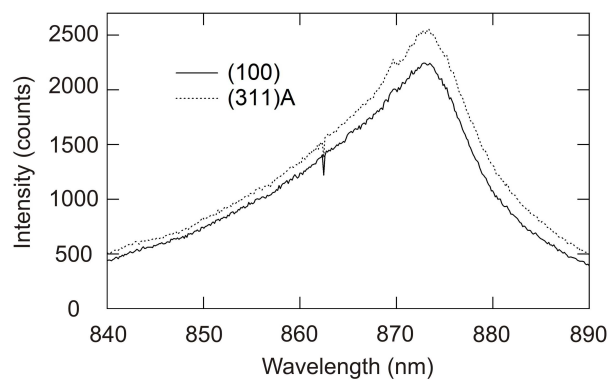


**Figure C1.** PL intensity vs wavelength for the two reference samples in section 3.2.

## References

- [1] Lebedev M V 2002 *Prog. Surf. Sci.* **70** 153
- [2] Liu D, Zhang T, LaRue R A, Harris Jr J S and Sigmon T W 1988 *Appl. Phys. Lett.* **53**,1059
- [3] Sandroff C J, Nottenburg R N, Bischoff J-C and Bhat R 1987 *Appl. Phys. Lett.* **51** 33
- [4] Yablonoitch E, Sandroff C J, Bhat R and Gmitter T 1987 *Appl. Phys. Lett.* **51** 439
- [5] Cohen R, Kronik L, Vilan A, Shanzer A and Cahen D 2000 *Adv. Mater.* **12** 33
- [6] Bessolov V N, Lebedev M V, Minh Binh N, Friedrich M and Zahn DRT 1998 *Semicond. Sci. Technol.* **13** 611
- [7] Hanein Y, Meirav U, Shahar D, Li C C, Tsui D C and Shtrikman H 1998 *Phys. Rev. Lett.* **80** 1288
- [8] Papadakis S J, De Poortere E P, Manoharan H C, Shayegan M and Winkler R 1999 *Science* **283** 2056
- [9] Tutuc E, Shayegan M and Huse D A 2004 *Phys. Rev. Lett.* **93** 036802
- [10] Clarke W R, Micolich A P, Hamilton A R, Simmons M Y, Hanna C B, Rodriguez J R, Pepper M and Ritchie D A 2005 *Phys. Rev. B* **71** 081304
- [11] Winkler R, Papadakis S, Poortere E D and Shayegan M 2000 *Phys. Rev. Lett* **85** 4574
- [12] Danneau R, Klochan O, Clarke W R, Ho L H, Micolich A P, Simmons M Y, Hamilton A R, Pepper M, Ritchie D A and Zülicke U 2006 *Phys. Rev. Lett* **97** 026403
- [13] Chen J C H, Klochan O, Micolich A P, Hamilton A R, Martin T P, Ho L H, Zülicke U, Reuter D and Wieck A D 2010 *New J. Phys* **12** 033043
- [14] Winkler R, Tutuc E, Papadakis S J, Melinte S, Shayegan M, Wasserman D and Lyon S A 2005 *Phys. Rev. B* **17** 195321
- [15] Danneau R, Klochan O, Clarke W R, Ho L H, Micolich A P, Simmons M Y, Hamilton A R, Pepper M and Ritchie D A 2008 *Phys. Rev. Lett.* **100** 016403
- [16] Yau J B, De Poortere E P and Shayegan M 2002 *Phys. Rev. Lett.* **88** 146801
- [17] Klochan O, Micolich A P, Hamilton A R, Trunov K, Reuter D and Wieck A D 2011 *Phys. Rev. Lett.* **107** 076805
- [18] Heiss D, Schaeck S, Huebl H, Bichler M, Abstreiter G, Finley J J, Bulaev D V and Loss D 2007 *Phys. Rev. B* **76** 241306
- [19] Burke A M, Waddington D E J, Carrad D J, Lyttleton R W, Tan H H, Reece P J, Klochan O, Hamilton A R, Rai A, Reuter D, Wieck A D and Micolich A P 2012 *Phys. Rev. B* **86** 165309
- [20] Jeong Y H, Choi K-H, Jo S-K and Kang B 1995 *Jpn. J. Appl. Phys.* **34** 1176
- [21] Li J V, Chuang S L, Aifer E and Jackson E M 2007 *Appl. Phys. Lett.* **90** 223503
- [22] Suyatin D B, Thelander C, Björk M T, Maximov I and Samuelson L 2007 *Nanotechnology* **18** 105307
- [23] Fan J-F, Oigawa H and Nannichi Y 1988 *Jpn. J. Appl. Phys.* **27** L2125
- [24] Nannichi Y, Fan J-F, Oigawa H and Koma A 1988 *Jpn. J. Appl. Phys.* **27** L2367
- [25] Besselov V and Lebedev M 1998 *Semiconductors* **32** 1141
- [26] Wang W I, Mendez E E, Kuan T S and Esaki L 1985 *Appl. Phys. Lett.* **47** 826
- [27] Sandroff C S, Hegde M S and Chang C C 1989 *J. Vac. Sci. Technol. B* **7** 841
- [28] Carpenter M S, Melloch M R and Dungan T E 1988 *Appl. Phys. Lett.* **53** 66
- [29] Sandroff C S, Hegde M S, Farrow L A, Chang C C and Harbison J P 1989 *Appl. Phys. Lett.* **54** 362
- [30] Sugahara H, Oshima M, Oigawa H, Shigekawa H and Nannichi Y 1991 *J. Appl. Phys.* **69** 4349
- [31] Paget D, Bonnet J E, Berkovits V L, Chiaradia P and Avila J 1996 *Phys. Rev. B* **53** 4604
- [32] Moriarty P, Murphy B, Roberts L, Cafolla A A, Hughes G, Koenders L and Bailey P 1994 *Phys. Rev. B* **50** 14237
- [33] Lu Z H, Graham M J, Feng X H and Yang B X 1993 *Appl. Phys. Lett.* **62** 2932
- [34] Scimeca T, Watanabe Y, Berrigan R and Oshima M 1992 *Phys. Rev. B* **46** 10201
- [35] Chadi D J 1985 *J. Vac. Sci. Technol. B* **3** 1167
- [36] Stiles K and Kahn A 1985 *J. Vac. Sci. Technol. B* **3** 1089

- [37] Sakata M and Ikoma H 1994 *Jpn J. Appl. Phys.* **33** 3813
- [38] Skromme B J, Sandroff C J, Yablonoitch E and Gmitter T 1987 *Appl. Phys. Lett.* **51** 2022
- [39] Hirayama H, Matsumoto Y, Oigawa H and Nannichi Y 1989 *Appl. Phys. Lett.* **54** 2565
- [40] Spindt C J, Liu D, Miyano K, Meissner P L, Chiang T T, Kendelewicz T, Lindau I and Spicer W E 1989 *Appl. Phys. Lett.* **55** 861
- [41] Sugahara H, Oshima M, Klauser R, Oigawa H and Nannichi Y 1991 *Surf. Sci.* **242** 335
- [42] Paget D, Gusev A O and Berkovits V L 1996 *Phys. Rev. B* **53** 4615
- [43] Berkovits V L, Bessolov V N, L'vova T N, Novikov E B, Safarov V I, Khasieva R V and Tsarenkov B V 1991 *J. Appl. Phys.* **70** 3707
- [44] Ivanov S V, Kop'ev P S and Ledentsov N N 1991 *J. Cryst. Growth* **108** 661
- [45] Chadi D J 1984 *Phys. Rev. B* **29** 785
- [46] Sugahara M, Oshima M, Oigawa H and Nannichi Y 1993 *J. Vac. Sci. Technol. A* **11** 52
- [47] Sugiyama M, Maeyama S and Oshima M 1994 *Phys. Rev. B* **50** 4905
- [48] Ohno T and Shiraishi K 1990 *Phys. Rev. B* **42** 11194
- [49] Sugiyama M, Maeyama S, Oshima M, Oigawa H, Nannichi Y and Hashizume H 1992 *Appl. Phys. Lett.* **60** 3247
- [50] Sugiyama M, Maeyama S and Oshima M 1993 *Phys. Rev. B* **48** 11037
- [51] Murphy B, Moriarty P, Roberts L, Cafolla T, Hughes G, Koenders L and Bailey P 1994 *Surf. Sci.* **317** 73
- [52] Ohno T 1991 *Phys. Rev. B* **44** 6306
- [53] Ren S-F and Chang Y-C 1990 *Phys. Rev. B* **41** 7705
- [54] Fan J-F, Oigawa H and Nannichi Y 1988 *Jpn. J. Appl. Phys.* **27** L1331
- [55] Sik H, Feurprier Y, Cardinaud C, Turban G and Scavenec A 1997 *J. Electrochem. Soc.* **144** 2106
- [56] Taguchi A and Shiraishi K 2005 *Phys. Rev. B* **71** 035349
- [57] Lu Z H, Chatenoud F, Dion M M, Graham M J, Ruda H E, Koutzarov I, Liu Q, Mitchell C E J, Hill I G and McLean A B 1995 *Appl. Phys. Lett.* **67** 670
- [58] Traub M C, Biteen J S, Brunschwig B S and Lewis N W, 2008 *J. Am. Chem. Soc.* **130** 955
- [59] Sandroff C J, Hegde M S, Farrow L A, Bhat R, Harbison J P and Chang C C 1990 *J. Appl. Phys.* **67** 586
- [60] Kuruvilla B A, Ghaisas S V, Datta A, Banerjee S and Kulkarni S K 1993 *J. Appl. Phys.* **73** 4384
- [61] Scimeca T, Watanabe Y, Maeda F, Berrigan R and Oshima M 1993 *Appl. Phys. Lett.* **62** 1667
- [62] Pashley M D and Li D 1994 *J. Vac. Sci. Technol. A* **12** 1848
- [63] Spindt C J and Spicer W E 1989 *Appl. Phys. Lett.* **55** 1653
- [64] Belkouch S, Aktik C, Xu H and Ameziane E L 1996 *Solid-state Electron.* **39** 507
- [65] Kane B E, Facer G R, Dzurak A S, Lumpkin N E, Clark R G, Pfeiffer L N and West K W 1998 *Appl. Phys. Lett.* **72** 3506
- [66] Clarke W R, Micolich A P, Hamilton A R, Simmons M Y, Muraki K and Hirayama Y 2006 *J. Appl. Phys.* **99** 023707
- [67] Grbić B, Leturcq R, Ensslin K, Reuter D and Wieck A D 2005 *Appl. Phys. Lett.* **87** 232108
- [68] Grbić B, Leturcq R, Ihn T, Ensslin K, Reuter D and Wieck A D 2007 *Phys. Rev. Lett.* **99** 176803
- [69] Komijani Y, Csontos M, Ihn T, Ensslin K, Reuter D and Wieck A D 2008 *Europhys. Lett.* **84** 57004
- [70] Csontos M, Komijani Y, Shorubalko I, Ensslin K, Reuter D and Wieck A D 2010 *Appl. Phys. Lett.* **97** 022110
- [71] Komijani Y, Csontos M, Shorubalko I, Ihn T, Ensslin K, Meir Y, Reuter D and Wieck A D 2010 *Europhys. Lett.* **91** 67010
- [72] Hinkle C L, Sonnet A M, Vogel E M, McDonnell S, Hughes G J, Milojevic M, Lee B, Aguirre-Tostado F S, Choi K J, Kim H C, Kim J and Wallace R M 2008 *Appl. Phys. Lett.* **92** 071901
- [73] Milojevic M, Hinkle C L, Aguirre-Tostado F S, Kim H C, Vogel E M, Kim J and Wallace R M 2008 *Appl. Phys. Lett.* **93** 252905